Postdoc Journal
Vol. 1 No. 2, February 2013

Journal of Postdoctoral Research
www.postdocjournal.com

Mechanical Instability of Thin Elastic Rods

Wanliang Shan*
The Department of Mechanical Engineering, Carnegie Mellon University, Pittsburgh, PA 15213, USA

Zi Chen†
Department of Biomedical Engineering, Washington University, St. Louis, MO 63130, USA

Mechanical instability of elastic rods has been subjected to extensive investigations and demonstrated fundamental roles in cytoskeletal mechanics and morphogenesis. Utilizing mechanical instability also has great potentials in engineering applications such as stretchable electronics. Here in this review, the fundamental theory underlying twisting and buckling instability of thin elastic rods is described. We then bridge together recent progresses in both theoretical and experimental studies on the topic. The promises and challenges in future studies of large deformation and buckling instability of thin rods are also discussed.

INTRODUCTION

The study of mechanical instability of rods can be dated back to Swiss mathematician Leonhard Euler in 1744 [1], and has been revived in the past few decades due to the ubiquitous and nontrivial nature of relevant phenomena. In fact, such nonlinear behaviors of rods are manifested in many systems both in nature and in engineering structures, including the growth of plant roots [2, 3], vines and tendrils [4], the mechanics of DNA [5], the twisting of tubes such as oil pipes [6–9], arteries and veins [10, 11], the twisting of cables such as stent guide wires [12, 13] and phone cords, nanoribbons and nanowires [14, 15], and the buckling of microtubules in cell cytoskeletons [16–18]. Fig. 1 shows some of these structures.

Euler did the first systematic study on planar buckling of rods [1], and proposed that buckling can occur with multiple wiggles (associated with an arbitrary mode number n), and the critical load scales as n^2. In reality, however, only mode 1 is energetically favorable in the absence of lateral support. Recently, Brangwynne et al. [16] showed that higher order modes appear when the rod is embedded in an elastic medium, leading to enhanced load bearing capability, which successfully explains the fact that microtubules act as the stiffest load-bearing filaments within cells.

The last two decades has seen increased interests in variants of this mechanics problem. For instance, buckling of rods or thin sheets with extra support from a surrounding medium received great attention due to potential application in bio-inspired design and soft/stretchable electronics [14, 15, 17–21]. In such a composite structure, the total free energy of the system under buckling load also incorporates that of the deformed surrounding medium. This extra support promotes the occurrence of higher order buckling modes predicted in conventional Euler buckling.

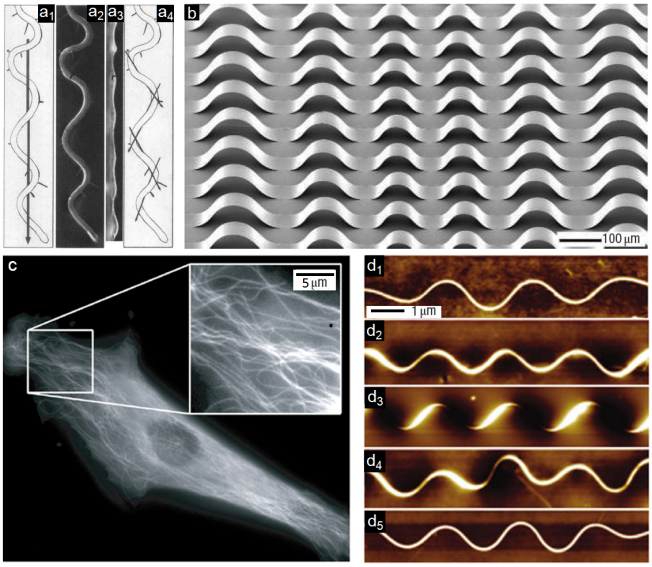

FIG. 1: **Buckling patterns in natural and engineering systems.** (a) Circumnutation models for the wavy-root of seedlings that grow on top of a tilted 1.5% agar medium. In one model, the root grows in a right-handed manner (a1), with the micrographs viewed from the top (a2) or from the right side (a3), while in the other model, each wave is formed alternatively by left-handed and right-handed parts (a4) [3]. (b) GaAs nanoribbons attached to pre-stretched PDMS substrate with patterned adhesive sites form buckling patterns under compressive loads [14]. (c) Buckling patterns of microtubules in a capillary cell that expresses EGFP-tubulin due to cell contractility (the inset being a high magnification image). Scale bar is 5 μm [16]. (d) AFM images of deformed Si NWs on the PDMS substrate at different treatment times of (d1) 0 min, (d2) 3 min, (d3) 5 min, (d4) 8 min, and (d5) 20 min. The prestrains were all set to be 20%. Scale bar is 1 μm [15]. Images (a) (b) (c) (d) adapted from [3], [14], [16], and [15], with permission from American Society of Plant Biologists (© American Society of Plant Biologists 1996), Nature Publishing Group (© Nature Publishing Group 2006), Rockefeller University Press, and American Chemical Society (© American Chemical Society 2011), respectively.

Another key topic is buckling of thin rods on the nanoscale [22–39]. As the applications of nanowires and nanotubes increase in nano-electrical mechanical systems and biotechnologies [40], such as AFM probes and shear sensors [41], there have been increasing investigations on the mechanical behavior of these nanoscale structures. When the length scale goes down to a few hundred nanometers or less, surface effects of the rod becomes non-negligible and have to be accounted for in the description of the total energy potential of the buckling rod [34–37, 42]. This effect often translates into size-dependent mechanical properties, which are typically distinct from those on the macro/micro scales [43–47].

In this review, we first present the classical theoretical description of elastic thin rod buckling. We then update on the recent theoretical and experimental progresses in the area of large deformation and buckling instability of thin elastic rods. Lastly, perspectives and concluding remarks are presented.

THEORY

First we give a quick review of the classical linear elasticity theory about large deformation and instability of rods, where Euler buckling is introduced as a special case for the general treatment. Here, the term "large deformation" refers to the large deformation where the strains are still small such that linear elasticity theory still applies. To gain a more comprehensive treatise, the readers are recommended to refer to the books by Landau and Lifshitz [1], Love [48] and Timoshenko [49].

Once the classical theory is set, we then move to the theoretical description for short wavelength buckling within medium providing linear and nonlinear elastic support and buckling of rods on the nanoscale.

Bending and twisting of rods

Following Landau and Lifshitz [1], we describe the general large deflection of Kirchhoff rods as a combination of bending and twisting (a Kirchhoff rod is assumed to be inextensible and unshearable). The rod is divided into infinitesimal elements, each bounded by the two adjacent cross sections. Within each element, a coordinate system $\{\mathbf{d}_x, \mathbf{d}_y, \mathbf{d}_z\}$ is designated such that in all the systems they are parallel in the undeformed configuration, and the $\mathbf{d}_z$ axes are along the tangent direction of the rod. As the rod deforms, these coordinate systems will rotate with respect to each other, and any two adjacent coordinate systems are rotated by an infinitesimal angle. Let $d\mathbf{Q}$ denote the vector of the relative angular rotation of two consecutive systems at a distance ds apart, and the rate of rotation is defined as $\mathbf{\Omega} = d\mathbf{Q}/ds$.

Take a unit vector $d\mathbf{t}$ tangential to the rod, then $d\mathbf{t}/ds$ is the curvature vector with the curvature $|d\mathbf{t}/ds| = 1/R$, where R denotes the local radius of curvature of the segment, and the direction is that of the principal normal ($\mathbf{n}$) to the curve at that point. The change of vector $\mathbf{t}$ between the two consecutive elements is equal to the cross product of the rotation vector and the vector $\mathbf{t}$ itself, $d\mathbf{t}/ds = \mathbf{\Omega} \times \mathbf{t}$. Take the vector product with $\mathbf{t}$ we get:

$$\mathbf{\Omega} = \mathbf{t} \times \frac{d\mathbf{t}}{ds} + \mathbf{t}(\mathbf{t} \cdot \mathbf{\Omega}) = \mathbf{t} \times \kappa\mathbf{n} + \tau\mathbf{t}, \tag{1}$$

where $\kappa = 1/R$ is the curvature and $\tau = \mathbf{t} \cdot \mathbf{\Omega}$ is the twist. In linear elasticity, the moment vector $\mathbf{M}$ has the following components, $M_1 = EI_1\kappa_1$, $M_2 = EI_2\kappa_2$, $M_3 = GJ\tau$, where I_1 and I_2 are the principal moments of inertia, J is the torsional moment of inertia and GJ denotes the twist rigidity of the rod. The elastic energy of the deflected rod is:

$$\begin{aligned} \Pi &= \int \left\{ \frac{1}{2} EI_1\kappa_1^2 + \frac{1}{2} EI_2\kappa_2^2 + \frac{1}{2} GJ\tau \right\} ds \\ &= \int \left\{ \frac{M_1^2}{2EI_1} + \frac{M_2^2}{2EI_1} + \frac{M_3^2}{2GJ} \right\} ds. \end{aligned} \tag{2}$$

Mechanical equilibrium of rods

We consider the equations of equilibrium of a deflected rod of length L. The force balance is given by $d\mathbf{T}/ds = -\mathbf{K}$, where $\mathbf{T}$ and $\mathbf{K}$ denote the internal resultant stress and the external force per unit length on the rod respectively, and s is the arclength (going from 0 to L). In equilibrium, the moment balance is described by $d\mathbf{M}(s)/ds = \mathbf{T} \times \mathbf{t}(s)$, where $\mathbf{M}(s)$ is the moment and $\mathbf{t}(s)$ denotes the tangent vector along the rod.

In the cases where the external forces are concentrated, i.e., the applied forces are only acting on discrete points of the rod, the equations can be greatly simplified. It can be shown that for a rod with a circular cross-section, the moment $\mathbf{M}(s)$ satisfies $\mathbf{M}(s) = EI\mathbf{t}(s) \times d\mathbf{t}(s)/ds + GJ\tau\mathbf{t}(s)$. When there are no twisting moments applied to the ends, the equation of equilibrium for pure bending can be simplified to:

$$EI \frac{d\mathbf{r}(s)}{ds} \times \frac{d^3\mathbf{r}(s)}{ds^3} = F \times \frac{d\mathbf{r}(s)}{ds}. \tag{3}$$

For small deflection of rods, the equations of equilibrium can be considerably simplified. The case considered here is when the direction of the tangent vector $\mathbf{t}$ to the rod varies very slowly along the length (i.e., the slope is very small). Typically, the radius of curvature is large

compared with the length of the rod, and the transverse displacement of the rod is much smaller than its length.

In the case where the rod is strongly compressed (under a force T exceeding a certain threshold), the governing equation is re-written in its component form (but neglecting F_x and F_y):

$$\begin{aligned} EI_2X'''' - TX'' - K_x = 0, \\ EI_1Y'''' - TY'' - K_y = 0. \end{aligned} \tag{4}$$

For a rod with hinged ends, the boundary conditions are $X = Y = 0, \quad X'' = Y'' = 0$, while for a rod with clamped ends, $X = Y = 0, \quad X' = Y' = 0$. Finally, for a free end, the force and moment have to vanish. Accordingly, the boundary conditions read $X'' = Y'' = 0, \quad X''' = Y''' = 0$.

Planar buckling instability of an elastic rod

When there are no transverse forces K_x and K_y, Eqns. (4) have the trivial solution $X = Y = 0$, suggesting that the rod remains straight under a longitudinal compressive force T. However, this solution only gives a stable equilibrium of the rod when the magnitude of the compressive force $|T|$ is below a certain threshold value T_c. When $|T| < T_c$, the straight rod is stable with respect to any small perturbation of the equilibrium shape. In other words, if the rod leaves the equilibrium shape by a small displacement, it has a natural tendency to go back to the original configuration to lower the total potential energy.

If, however, $|T| > T_c$, the straight configuration becomes unstable. Any small perturbation will suffice to disrupt the equilibrium configuration, resulting in a non-negligible bending of the rod with a new equilibrium shape. When $|T| = T_c$, the straight shape of the rod is in neutral equilibrium, which suggests that there are also states where the rod is bent slightly but still in mechanical equilibrium besides the straight configuration. Therefore, the critical value, T_c, is the value of $|T|$ such that there exists a non-trivial solution for the following equations:

$$EI_2X'''' + |T|X'' = 0, \quad EI_1Y'''' + |T|Y'' = 0. \tag{5}$$

This solution also depicts the shape of the deformed rod in a new equilibrium state after it ceases to remain straight.

Now we consider the classical problem of buckling, i.e., what is the critical compression force for a rod with hinged ends. An alternative description is to seek the smallest value of $|T|$ such that Eqns. (5) possess a non-trivial solution. Hence it suffices to consider just the equation that contains the smaller of I_1 and I_2. Without a loss of generality, suppose $I_2 < I_1$, then we may seek a solution of the equation $EI_2X'''' + |T|X'' = 0$ in the form $X = A + Bz + C\sin qz + D\cos qz$, where $q = \sqrt{|T|/EI_2}$. For conciseness, we drop the subscript "2" hereafter. The non-zero solution which satisfies the boundary conditions $X = X'' = 0$ for $z = 0$ and $z = l$ is $X = C\sin qz$. Thereby we find that the critical force for the Euler buckling load with hinged boundary conditions is $T_c = \frac{\pi^2 EI}{L^2}$. If both ends are clamped, then in a similar fashion, the critical force can be derived to be $T_c = 4\pi^2 EI/L^2$. Thus the critical buckling load can be written as:

$$T_c = \eta\frac{\pi^2 EI}{L^2}, \tag{6}$$

where η depends on the boundary and loading conditions.

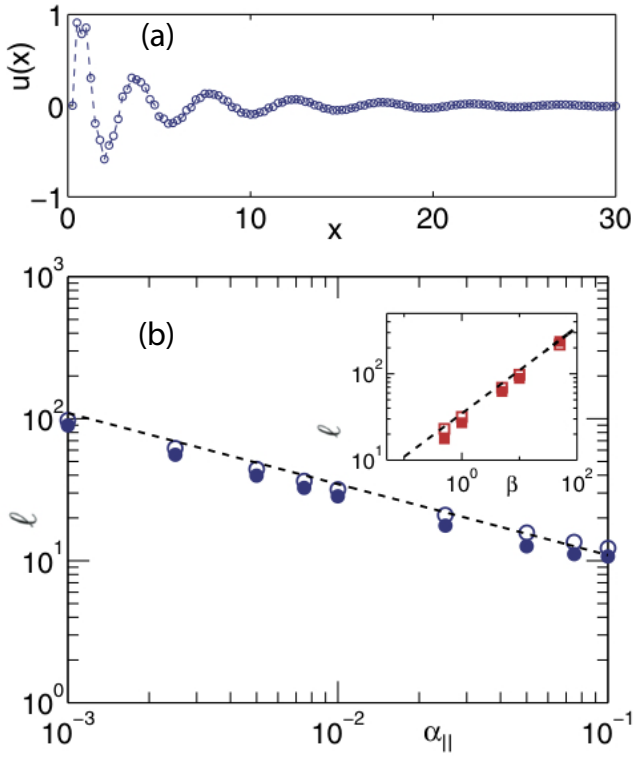

FIG. 2: **Numerical results of the deformation of a stiff elastic rod embedded in a nonlinearly elastic medium.** (a) The exponentially decaying buckling pattern. (b) the decay length as a function of the longitudinal coupling parameter, $\alpha_{\|}$ and the bending rigidity κ [17]. Reproduction of images (a), (b) from [17] with permission from IOP Science (© IOP Science 2008).

Planar Buckling instability of a rod in elastic media

For a rod that sustains compressive loading from one end and buckles in an elastic medium, one can write down the

energy functional for small deflections [17]:

$$\Pi = -fv(0) + \int_0^\infty [\frac{\kappa}{2}u''^2(x) + \frac{1}{2}\alpha_\perp u^2(x) + \frac{1}{2}\alpha_\parallel v^2(x) + \frac{1}{4}\beta u^4(x)]\mathrm{d}x, \tag{7}$$

where f is a compressive load imposed at the free end ($x = 0$), $u(x)$ and $v(x) = \int_x^\infty \mathrm{d}s\frac{1}{2}u'(s)^2$ denote the rod's transverse and longitudinal displacements, respectively. The elastic coupling parameters $\alpha_\perp$ and $\alpha_\parallel$ are dictated by the rod's dimensions and the gel's elastic properties. For a straight rod of length L embedded in an elastic medium, $\alpha_\perp \approx 4\pi G/\ln(2L/d)$ and $\alpha_\parallel = \alpha_\perp/2$ [50, 51] are the transverse and longitudinal coupling coefficients respectively, and β is the coupling constant for the nonlinear elastic energy.

Based on this model, Das et al. [17] theoretically investigated the mechanical buckling of an elastic filament embedded in a non-linear elastic medium and the associated force propagation. Inspired by the numerical results (Fig. 2a), an exponentially decaying ansatz for the buckling amplitude $u(x)$ can be assumed as follows:

$$u(x) = u_0 \exp(x/\ell) \sin\frac{2\pi x}{\lambda}, \tag{8}$$

where ℓ is the decay length and λ is the buckling wavelength. It is shown that reinforced microtubules buckle when their compressive load exceeds a critical value, consistent with the previous experiments [16]. Moreover, the resulting deformation is mostly limited to a penetration depth, ℓ, depending on the coupling between the filament and the cytoskeleton $(\alpha_\parallel, \alpha_\perp)$, as well as the non-linear mechanical properties of the surrounding matrix (β). The buckling amplitude goes with the applied load f as $(f - f_c)^{1/2}$, while the penetration depth (or decay length ℓ) scales as $(\beta/\alpha_\parallel)^{1/2}$ (Fig. 2b).

Very recently, Shan et al. [21] furthered this investigation by varying the magnitude of the nonlinearity in elasticity (β), from significant to small. The numerical simulation results show that in this linear regime, a decay length still exists and scales as $(\kappa/\alpha_\parallel)^{1/4}$, where κ denotes the bending rigidity of the rod [21]. They hence identified a short wavelength buckling regime that is governed mainly by the linear elasticity effect when the nonlinear medium property (β) becomes negligible. Based on the linear model, the exponentially decaying buckling profile was found to relate to the external loading in the following manner:

$$f - f_c \approx \frac{1}{2}\alpha_\parallel \ell v(0), \tag{9}$$

where $v(0)$ is the displacement at the loading end of the thin elastic rod.

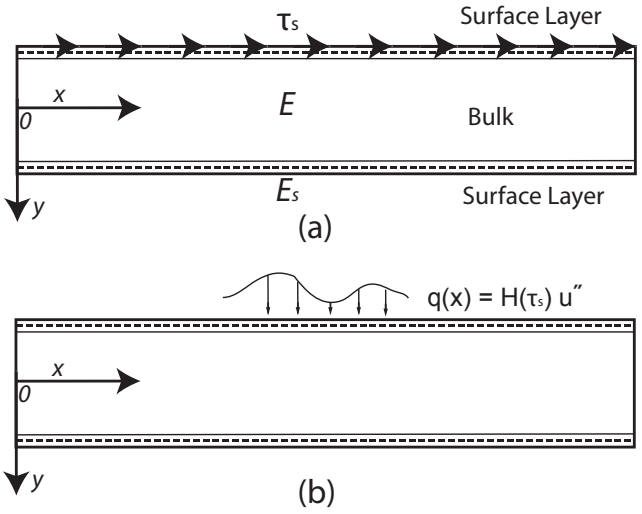

FIG. 3: **Residual surface stress (a) causes distributed stresses (b) on the buckling nanowire** [42]. Images adapted from [42] with permission from American Institute of Physics (© American Institute of Physics 2007)

Planar buckling instability of a rod on the nanoscale

On the nanoscale, the effects of surfaces on buckling, bending and other mechanical properties can be described by surface energy or surface stress. The surface stress tensor $\sigma^s_{\alpha\beta}$ is related to the surface energy density γ in the following manner [52, 53]:

$$\sigma^s_{\alpha\beta} = \gamma\delta_{\alpha\beta} + \frac{\partial\gamma}{\partial\epsilon^s_{\alpha\beta}}; \quad \text{or in 1D,} \quad \tau_s = \tau^0 + E^s\epsilon. \tag{10}$$

where $\epsilon^s_{\alpha\beta}$ is the surface strain tensor, τ_0 is the residual surface stress and E^s is the surface Young's modulus. Note that in the simplified 1D case, γ has been assumed to be a single-valued function of ϵ, which introduces the concept of surface elasticity [54].

By idealizing a surface with zero thickness but possessing a surface elasticity characterized by E^s, Wang et al. came up with an effective flexural rigidity $(EI)^*$ for nanorods [34, 46]. The difference between $(EI)^*$ and the original (EI) is determined by E^s and other geometrical parameters related to the cross section of the rod. The authors then used Laplace-Young equation to describe the jump of the normal stress across the elastic surface $< \sigma^+_{ij} - \sigma^-_{ij} > n_i n_j$ and obtained the distributed transverse loading induced by the residual surface tension in 1D [34]:

$$q(x) = H\frac{\partial^2 u}{\partial x^2}, \tag{11}$$

where u is the transverse displacement as earlier defined and H is a constant determined by τ^0 and other geomet-

rical parameters associated with the cross section. Fig. 3 shows an example of the stress distribution of such an idealized nanowire with residual surface stresses.

Thus, the governing equation for the nanobeam buckling is updated from Eqn. (5) to the following form:

$$(EI)^* \frac{\partial^4 u}{\partial x^4} + (T - H)\frac{\partial^2 u}{\partial x^2} = 0. \tag{12}$$

The solution to Eqn. (12) is similar to that of the conventional Euler buckling in Eqn. (6):

$$T_c^s = \eta \frac{\pi^2 (EI)^*}{L^2} + H. \tag{13}$$

E^s and τ_0 may be negative or positive, and can be obtained using atomic simulations [43, 55]. Thus, depending on the sign of these parameters, T_c^s may be larger or smaller than T_c. The same holds for the estimation of Young's modulus from nanobeam buckling using conventional Euler buckling formulation.

EXPERIMENTAL STUDIES

Buckling in elastic media

Brangwynne et al. [16] showed that intracellular microtubules can bear enhanced compressive loads when the buckling wavelength is significantly reduced due to elastic support of the surrounding cytoskeleton matrix. In this pioneering study, a quantitative model was proposed to interpret this behavior, which shows that the transverse coupling has dramatically enhanced the compressive loads that microtubules can bear, implying that they can contribute more significantly to the mechanical properties of the cell than previously considered possible. As has been derived in the Theory section, Euler buckling of a thin rod of length L under an axial compression occurs at a critical load, f_c. If the rod is embedded in an elastic medium, however, the deformation energy of the medium should also be taken into account. More specifically, the elastic support of a medium with a shear modulus, G, can reduce the buckling wavelength to $\lambda \sim (\kappa/G)^{1/4}$ because of the competition between the deformation energy of a rod with bending rigidity κ and the elastic energy in the medium due to the rod's deflections [1]. Correspondingly, the critical force f_c also increases.

In addition to the theoretical contribution aforementioned, Shan et al. [21] also further studied the buckling behavior of thin elastic rods reinforced by a biopolymer matrix through experiments. It is shown that the attenuated buckling of thin rods reinforced by an elastic matrix can be accounted for by a linear model

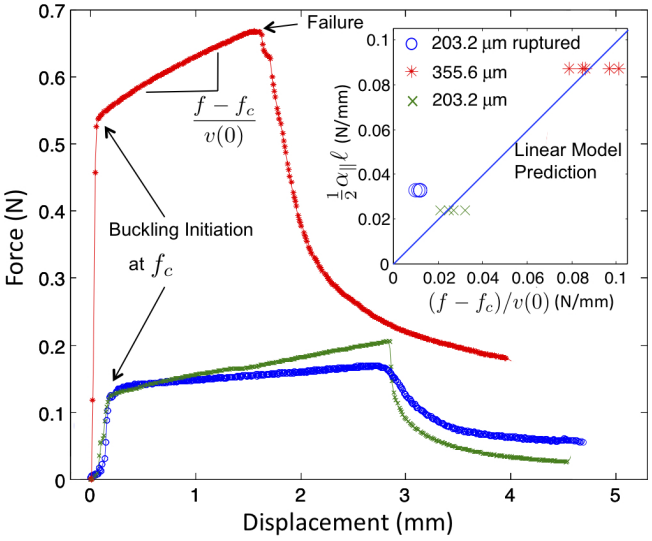

FIG. 4: **Load vs displacement curves for short wavelength buckling of nitinol wires embedded in gelatin.** The excellent agreement of loading curve slopes $(f - f_c/v(0))$ with predictions from linear model $\alpha\ell/2$ verified the validity of the proposed model [21].

which quantifies the no-slip coupling between the rod and medium. Here, the decay length is shown to be controlled merely by the linear longitudinal coupling to the medium and the rod's bending rigidity, which goes in contrast with the previous work which identified a regime where the nonlinear response of the medium controlled the penetration depth [17]. The experimental results support that the linear model captures the main features of the buckling behavior investigated here (Fig. 4). In addition, it is also identified, in this work, a dynamic behavior where the rod and the medium can be partially uncoupled, and that the effective nonlinearities result from the stick-slip behavior at the interface, thus revealing a rich and complex dynamic behavior of the rod-gel interface.

Mechanical buckling also plays an important role in the growth of some plant roots. For example, Silverberg et al. [51] recently found that the roots of *Medicago truncatula* grown in a transparent hydrogel of two layers of different stiffness deformed helically just above the upper gel layer interface. This phenomena has been shown to result from growth-induced buckling in the medium accompanied by a spontaneous twist near the growing root tip. The helical morphology is shown to vary with the modulus of the upper gel layer and demonstrate that the size of the deformation varies with gel stiffness as expected by a mathematical model based on the theory of buckled rods.

Buckling on the nanoscale

Experiments of buckling on the nanoscale typically involve nano-mechanical systems to achieve accurate positioning and application/measurement of mechanical loading on the scale of nano Newtons. These nano-mechanical systems include AFM probes, Nano-indenters and many other custom-designed systems [22, 25, 38, 39]. The nanobeams or nanowires are typically grown on a rigid substrate. Indenters, or other probes, can be driven to approach the free end of the nanobeam to apply mechanical loading. By measuring the buckling profile and tracking the buckling loads, these experiments on nanwires and nanorods have been used to estimate the mechanical properties of the corresponding materials on nano scale and make comparison with those on the macro scale.

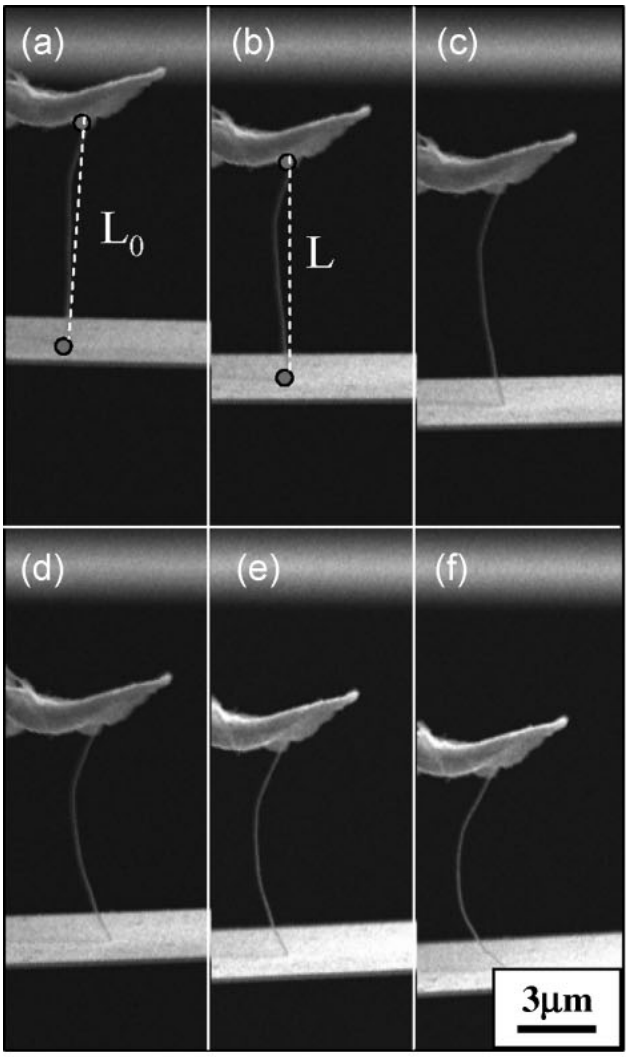

FIG. 5: **A series of snapshot SEM images showing the continuous buckling of the Si nanowire using an AFM probe** [38]. Reproduction of images (a-f) from [38] with permission from Wiley (© Wiley 2008)

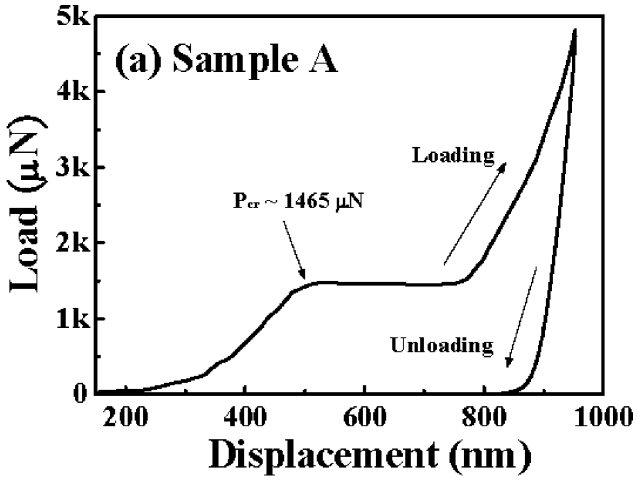

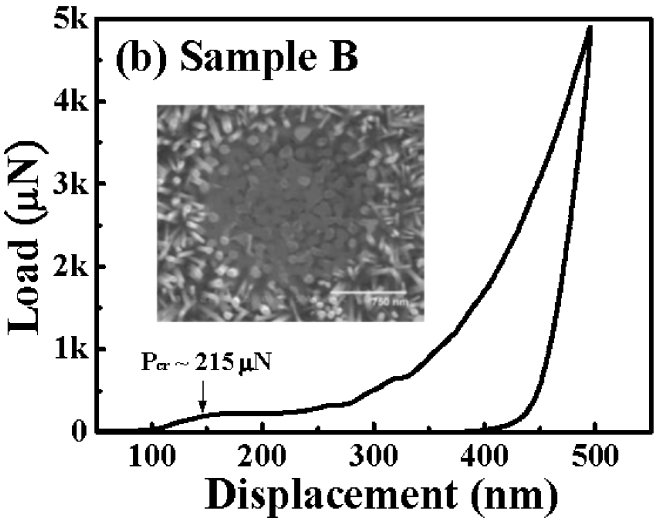

FIG. 6: **Load vs displacement curves for buckling of ZnO nanowires by nanoindentation technique.** The inset shows the top view of the deformation zone after indentation [25]. Reproduction of images (a), (b) from [25] with permission from American Institute of Physics (© American Institute of Physics 2007)

For instance, Hsin et al. investigated the buckling and bending of Silicon nanowires using a manipulation probe and an Atomic Force Microscope (AFM) tip within a Scanning Electron Microscope (SEM) (Fig. 5) [38]. The nanowires in this work were fabricated by a chemical vapor deposition procedure. Using the conventional Euler buckling theory, they estimated the Young's modulus of Silicon nanowire and found that it's consistent with the bulk value. Thus the elastic modulus was not changed by the reduction to a nanometer scale. Similar result was found for gold nanowires through direct contact buckling using AFM probes within a SEM [39].

Ji et al. studied the buckling of Zinc oxide nanowires under uniaxial compression, using nanoindentation

technique [25]. These nanowires were grown on ZnO:Ga/glass templates, with different diameters and lengths, as denoted in Fig. 6, where sample A had a length of 2000 nm and a diameter of 100 nm, while sample B had a length of 800 nm and a diameter of 30 nm. The Force-Displacement curves were shown in Fig. 6 for these samples. These curves showed a distinct critical load for buckling initiation, which was used for the estimation of Young's modulus of ZnO nanowires based on the conventional Euler buckling theory. It was found that the Young's modulus estimated from these buckling experiment exhibited a strong size-dependent effect, where the shorter and slender sample B had a much larger E. In addition, the estimations of E for both nanowires were larger than that of the single crystal bulk wurtzite. The authors attributed this to the potential roles of surface effects because of the large surface-to-volume ratio. However, similar work on ZnO nanowire by Riaz et al. reported a much smaller Young's modulus estimated from Johnson model instead of a conventional Euler model [22].

These experimental findings verified the theory of surface effects analyzed in earlier sections. Depending on the surface elasticity constant and the residual surface stress, the Young's modulus may be overestimated or underestimated if using Euler's theory directly on buckling of nanowires.

PERSPECTIVES AND CONCLUDING REMARKS

While the large deformation and mechanical instability in rod-like structures have been extensively studied, many relevant, interesting problems remain to be investigated.

First, there are some mathematical complications in modeling buckling and post-buckling of thin structures that remain to be dealt with. For example, even in the case of planar buckling of a rod embedded in an elastic matrix, analytic solution has not hitherto been achieved, not to mention the more complicated scenario of helical buckling [51], where the mechanics is highly nonlinear.

Second, the mechanical instability of materials, especially biological materials, is often associated with material inhomogeneity and nonlinearity. In particular, exploring the role of mechanical instability in the morphogenesis of living tissues and organs [56, 57] represents new challenges to engineers. For example, not only does mechanical buckling have significant implications in addressing cytoskeletal mechanics, but also it plays an important role in the morphogenesis of tortuous veins often observed in a variety of diseases, such as venous hypertension and diabetic retinopathy, whereby the underlying mechanisms of vein tortuosity remain poorly understood [58, 59]. Moreover, the buckling of bio-filaments with thermal (entropic) effects presents rich and complex behaviors [60–63], with significant relevance in understanding the mechanical properties of filament networks [64] and cellular processes such as mechanotranduction and cytokinesis [65].

Third, extending the study of mechanical buckling in rods to address instability in thin sheets and soft materials has received increasing attention [57, 67–69], where geometric nonlinear effects [66] can play an important role even for mechanically homogenous materials, adding to the complexity in mathematically modeling the mechanical behavior of such nonlinear systems. Here the coupling between geometric and material nonlinearities can lead to interesting new phenomena that deserve further theoretical and experimental investigations.

Last but not least, exploiting mechanical instabilities and turning failure into use, such as in designing flexible and stretching electronics [14], can lead to development of new technology with broad applications in engineering. In this review, we have mainly limited discussions to buckling of rod structures, while the buckling, wrinkling, and creasing of planar and bulk structures [70] open up plenty of venues for both theoretical and experimental investigations, with a broad spectrum of engineering applications.

ACKNOWLEDGMENTS

Z. Chen acknowledges the support by the Society in Science - Branco Weiss fellowship, administered by ETH, Zurich.

* wlshan@cmu.edu
† chen.z@seas.wustl.edu

[1] L. D. Landau and E. M. Lifshitz, Theory of Elasticity, 1986, Pergamon Press, Oxford.
[2] L. Okada and Y. Shimura. Science, 1990, 250, 274-276.
[3] R. Rutherford and P. H. Masson, Plant Physiol. 1996, 111, 987-998.
[4] A. Goriely and S. Neukirch. Phys. Rev. Lett. 2006, 97, 184302.
[5] Y. Snir and R. D. Kamien. Science, 2005, 307, 1067.
[6] J. C. Cunha, SPE Drill Completion, 2004, 19, 13-19.
[7] N. C. Huang and P. D. Pattillo, Int. J. Nonlinear Mech. 2000, 35, 911-923.
[8] J. Wu and H. C. Juvkam-Wold, Trans. ASME, 1993, 115, 196-201.
[9] J. Wu, H. C. Juvkam-Wold and R. Lu, Trans. ASME, 1993, 115, 190-195

[10] H. C. Han, J Biomech, 2007, 40(16), 3672-2678.
[11] H. C. Han, J Biomech, 2008, 41(12), 2708-2713.
[12] P. A. Schneider, Endovascular skills: guidewire and catheter skills for endovascular surgery, 2003, NY: Dekker, New York.
[13] J. S. Chen and H. C. Li, Transactions of ASME, 2011, 78, 041009.
[14] Y. Sun, W. M. Choi, H. Jiang, Y. Y. Huang and J. A. Rogers, Nature Nanotech. 2006, 1, 201-207.
[15] F. Xu, W. Lu, and Y. Zhu, ACS Nano 2011, 5, 672-678.
[16] C. P. Brangwynne, F. C. MacKintosh, S. Kumar, L. Mahadevan, N. Geisse, K. K. Parker, D. E. Ingber and D. A. Weitz, J Cell Biology, 2006, 173, 733-741.
[17] M. Das, A. J. Levine, F. C. MacKintosh, Europhysics Letters, 2008, 84, 18003.
[18] T. Li, Journal of Biomechancis, 2008, 41, 1711-1729.
[19] D. H. Kim, J. Song, W. M. Choi, H. S. Kim, R. H. Kim, Z. Kiu, Y. Y. Huang, K. C. Hwang, Y. W. Zhang and J. A. Rogers. PNAS, 2008, 105(48), 18675-18680.
[20] J.A. Rogers, T. Someya and Y.G. Huang, Science, 2010, 327, 1603-1607.
[21] W. L. Shan, Z. Chen, C. P. Broedersz, A.A. Gumaste, W. O. Soboyejo, C. P. Brangwynne, Soft Matter, 2013, 9, 194-199.
[22] M. Riaz, O. Nur, M. Willander and P. Klason, Appl. Phys. Lett. 2008, 92, 103118.
[23] R. Gunawidjaja, H. Ko, C. Jiang and V. V. Tsukruk, Chem. Mater., 2007, 19, 2007-2015.
[24] P. A. T. Olsson and H. S. Park, Acta Materialia, 2011, 59, 3883-3894.
[25] L. W. Ji, S. J. Young, T. H. Fang and C. H. Liu, Appl. Phys. Lett., 2007, 90, 033109.
[26] C. H. Lin, H. Ni, X. Wang, M. Chang, Y. J. Chao, J. R. Deka and X. Li, Small, 2010, 6(8), 927-931.
[27] Y. Zhu, Q. Qin, Y. Gu and Z. L. Wang, Nanoscale Res. Lett. 2010, 5, 291-195.
[28] S. J. Young, L. W. Ji, S. J. Chang, T. H. Fang, T. J. Hsueh, T. H. Meen and I. C. Chen. Nanotechnology, 2007, 18, 225603.
[29] B. Li, Q. Zhao, H. Huang, Z. Luo, M. K. Kang, J. H. Im, R. A. Allen, M. W. Cresswell, R. Huang and P. S. Ho, J. Appl. Phys., 2009, 105, 073510.
[30] J. Xiao, S. Y. Ryu, Y. Huang, K. C. Hwang, U. Paik and J. A. Rogers, Nanotechnology, 2010, 12, 085708.
[31] T. Murmu and S. C. Pradhan, Physica E, 2009, 1232-1239.
[32] A. T. Samaei, M. Bakhtiari and G. F. Wang. Nanoscale Research Letters, 2012, 7, 201.
[33] H. Yao and G. Yun, Physica E, 2012, 44, 1916-1919.
[34] G. F. Wang and X. Q. Feng, Appl. Phys. Lett. 2009, 94, 141913.
[35] G. F. Wang and X. Q. Feng, J. Phys. D: Appl. Phys. 2009, 42, 155411.
[36] G. F. Wang and Fan Yang, J. Appl. Phys. 2011, 109, 063535.
[37] J. S. Wang, X. Q. Feng, G. F. Wang and S. W. Yu, Appl. Phys. Lett. 2008, 92, 191901.
[38] C. L. Hsin, W. Mai, Y. Gu, Y. Gao, C. T. Huang, Y. Liu, L. J. Chen and Z. L. Wang, Adv. Mater. 2008, 20, 3919-3923.
[39] W. J. Kim, S. M. Carr and M. N. Wyboume, Appl. Phys. Lett. 2005, 87, 173112.
[40] Y. Cui, Z. H. Zhong, D. L. Wang, W. U. Wang and C. M. Lieber, Nano. Lett. 2003, 3, 149.
[41] C. Pang, G. Y. Lee, T. Kim, S. M. Kim, H. N. Kim, S. H. Ahn and K. Y. Suh, Nature Materials, 2012, 11, 795-801.
[42] G. F. Wang and X. Q. Feng, Appl. Phys. Lett. 2007, 90, 231904.
[43] R. E. Miller and V. B. Shenoy, Nanotechnology, 2000, 11, 139-147.
[44] S. Cuenot, C. Fretigny, S. Demoustier-Champagne and B. Nysten, Phys. Rev. B, 2004, 69, 165410.
[45] C. Q. Chen, Y. Shi, Y. S. Zhang, J. Zhu and Y. J. Yan, Phys. Rev. Lett. 2006, 96, 165410.
[46] J. He and C. M. Lilley, Nano. Lett. 2008, 8, 1798.
[47] X. P. Zheng, Y. P. Cao, B. Li, X. Q. Feng and G. F. Wang, Nanotechnology, 2010, 21(20), 205702.
[48] A. E. H. Love. A Treatment On the Mathematical Theory of Elasticity, 4th ed, 1944, Dover Publications, New York.
[49] S. Timoshenko and S. Wonowsky-Krieger. Theory of Plates and Shells, 1959, McGraw-Hill.
[50] A. J. Levine, T. B. Liverpool and F. C. MacKintosh, Phys. Rev. E, 2004, 69, 021503.
[51] J. L. Silverberg, R. D. Noar, M. S. Packer, M. J. Harrison, C. L. Henley, I. Cohen and S. J. Gerbode, PNAS, 2012, 16794-16799.
[52] J. W. Gibbs, The Scientific Papers of J. Willard Gibbs, Vol. 1: Thermodynamics, 1906, Longmans and Green, New York.
[53] R. C. Cammarata, Prog. Surf. Sci. 1994, 46, 1.
[54] M. E. Gurtin, J. Weissmuller and F. Larche, Philos. Mag. A 1998, 78, 1093.
[55] V. B. Shenoy, Phys. Rev. B, 2005, 71, 094104.
[56] M. A. Wyczalkowski, Z. Chen, B. Filas, V. Varner and L. A. Taber, Birth Defects Res., Part C, 2012, 96, 132.
[57] Z. Liu, S. Swaddiwudhipong, and W. Hong. Soft Matter, 2013, 9, 577-587.
[58] R. Martinez, C. A. Fierro, P. K. Shireman, and H. C. Han. Ann Biomed Eng. 2010, 38(4), 1345-353.
[59] H. C. Han, J. Vasc. Res. 2012, 49(3), 185-197.
[60] K. Baczynski, R. Lipowsky and J. Kierfeld, Phys. Rev. E, 2007, 76(6), 061914.
[61] M. Emanuel, H. Mohrbach, M. Sayar, H. Schiessel and I. M. Kulic, Phys. Rev. E, 2007, 76(6), 061907.
[62] J. R. Blundell and E. M. Terentjev, J. Phys. A: Math. Theor. 2007, 40, 10951.
[63] B. Hu, V.B. Shenoy, and Y. Lin. J. Mech. Phys. Solids, 2012, 60, 1941-1951.
[64] M. P. Murrell and M. L. Gardel. PNAS Early Edition. DOI: 10.1073/pnas.1214753109.
[65] T. D. Pollard, Curr. Opin. Cell Biol. 2010, 22(1), 50-56.
[66] Z. Chen, Q. Guo, C. Majidi, W. Chen, D. J. Srolovitz, and M. P. Haataja. Phys. Rev. Lett. 2012, 109, 114302.
[67] J. Huang, B. Davidovitch, C. D. Santangelo, T. P. Russell and N. Menon, Phys. Rev. Lett., 2010, 105, 038302.
[68] J. Kim, J. A. Hanna, M. Byun, C.D. Santangelo and R.C. Hayward. Science, 2012, 335, 1201-1205.
[69] L. Pocivavsek, R. Dellsy, A. Kern, S. Johnson, B. Lin, K. Y. C. Lee, and E. Cerda, Science, 2008, 320, 912.
[70] B. Li, Y. Cao, X. Feng and H. Gao. Soft Matter, 2012, 8, 5728-5745.